Ferrofluid Moving Thin Films for Active Flow Control

Francisco J. Arias[a]*
[a] *Department of Fluid Mechanics, Polytechnic University of Catalonia,*
ESEIAAT C/ Colom 11, 08222 Barcelona, Spain
(Dated: July 15, 2020)

Ferrofluid moving thin films and its possible significance with regard to active flow control for lift enhancement is discussed. In this strategy, a very thin film of ferrofluid is strongly attached at the wall of the wing by a normal magnetic field from below and pumped tangentially along the wing. As a result, the zero slip condition is eliminated between the surface of the wing and the air stream and simulating all the effects of a moving wall leading in the appearance of slip velocity in the air-ferrofluid interface including the injection of momentum into the boundary layer. Utilizing a simplified physical model and from the available experimental data on moving walls, the expected lift enhancement and effect on the attack angle was assessed. Additional R&D is required in order to explore the possibilities in the use of ferrofluid moving thin films.

Keywords. *Ferrofluid; Boundary layer separation; Active flow control*

I. INTRODUCTION

The wing aerodynamic performance is frequently reduced by the detachment of the boundary layer. Active control flow are a variety of flow control strategies aimed to decrease the drag or increase the lift by affecting the separation of the boundary layer which require a certain energy input. A variety of novel flow control strategies have been proposed almost immediately after the Prandtl introduced his boundary layer theory in 1904 to understand the flow behavior of a viscous fluid near a solid boundary some of which include the suction and blowing, turbulence promoters, vortex generator, synthetic jets, and moving walls. [1]-[9], and today active control flow is an active research topic,[10]-[15].

The object of this work was to analyze a novel approach for lift enhancement and flow control. In this concept, the goal is attained by preventing the growth of the boundary layer from the elimination of the zero slip condition between the surface and the air stream. The concept would simulate all effects of a moving wall leading in the appearance of slip velocity in the gas-fluid interface including the injection of momentum into the boundary layer, with one exception: there is no moving wall but instead a ferrofluid thin film attached at the wall by a magnetic field. For this work, suffice is to know that a ferrofluid or ferromagnetic fluid is nothing more than a colloidal liquid that becomes strongly magnetized in the presence of a magnetic field due to presence of nanoscale ferromagnetic, or ferrimagnetic, particles suspended. Fig. 1 shows a pictorially illustration of the core idea proposed in this work.

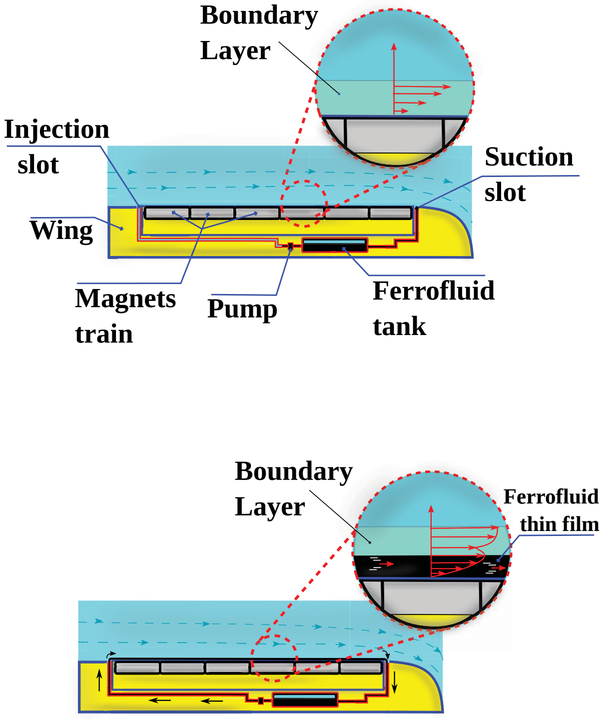

FIG. 1: Top: zero slip condition limit the maximum maximum attack angle and lift of the wing. Bottom: a ferrofluid moving film eliminates the zero slip condition and injecting momentum into the boundary layer.

II. MATERIALS AND METHODS

A. The ferrofluid moving thin film

Let us consider Fig. 2 in which a ferrofluid thin film with a thickness δ is strongly attached at the wall of the wing by a magnetic field from below and normal to its surface (z co-ordinate). At the same time, the film is

---

*Corresponding author: Tel.: +93 73 98 666; Electronic address: `francisco.javier.arias@upc.edu`

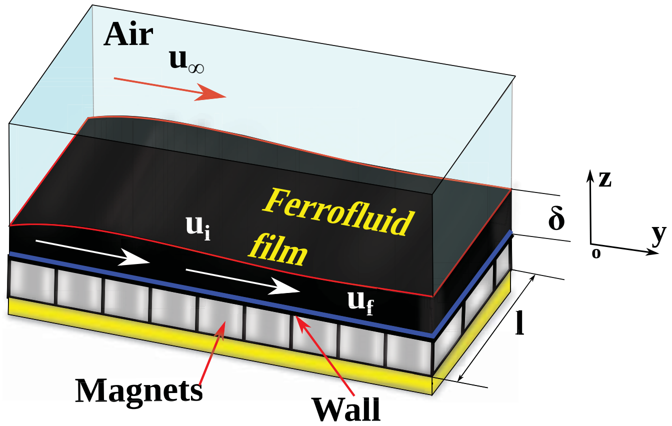

FIG. 2: Physical model of the region of the airfoil covered by the ferrofluid film

tangentially pumped along the wing (y co-ordinate) with an average velocity u_f and transmitting momentum into the air-ferrofluid interface. It is desired to know what is the velocity at the interface air-ferrofluid as function of the average velocity of the ferrofluid layer.

Because the ferrofluid layer is very thin, and its velocity can be regarded as totally parallel to the wall, then it is allowable to assume a simple Couette flow with a certain pressure gradient along the wall (responsible to pump the fluid), [16]

$$u(z) = -\frac{1}{2\mu_f}\frac{dp}{dy} z\left(\delta - z\right) + u_i\frac{z}{\delta} \tag{1}$$

where $u(z)$ is the velocity of the fluid (in the y-direction) at a distance z from the flow; μ_f the ferrofluid viscosity; $\frac{dp}{dy}$ the pressure gradient along the wall; u_i the velocity at the interface air-ferrofluid; and δ the ferrofluid film thickness. Expression, Eq.(1) accomplishes the boundary condition at the interface $u(z=\delta)=u_i$ and the zero slip condition at the wall $u(z=0)=0$.

The average velocity is calculated as

$$\bar{u} = \frac{1}{\delta}\int_o^\delta u(z)dz \tag{2}$$

where l is the length of the film. Inserting Eq.(1) and after integration yields,

$$\bar{u} = -\frac{1}{2\mu_f}\frac{dp}{dy}\frac{\delta^2}{6} + \frac{u_i}{2} \tag{3}$$

There is a final boundary condition which is related with the need for continuity of the stress component tangential at the interface ferrofluid-air

$$\mu_f\left.\frac{\partial u}{\partial z}\right|_{z=\delta} + \mu_a\left.\frac{\partial v}{\partial z}\right|_{z=\delta} = 0 \tag{4}$$

where v and μ_a are the air velocity and dynamic viscosity, respectively.

Considering that $\mu_f \gg \mu_a$, then if it is allowable to assume $\mu_f\frac{\partial u}{\partial z} \gg \mu_a\frac{\partial v}{\partial z}$ and then Eq.(4) simplify as

$$\mu_f\left.\frac{\partial u}{\partial z}\right|_{z=\delta} \approx 0 \tag{5}$$

Applying Eq.(1) into Eq.(5) yields

$$-\frac{1}{2\mu_f}\frac{dp}{dy} = \frac{u_i}{\delta^2} \tag{6}$$

which inserted into Eq.(3) one obtains

$$\bar{u} = \frac{2u_i}{3} \tag{7}$$

B. Film stability

According with Eq.(7), one may be tempted to think that by increasing the volumetric flow and then the average velocity $\bar{u}$ it can be increased linearly the interface velocity u_i and then the injection of momentum into the boundary layer of the air. However, this is not the case, and the maximum interface velocity is limited by Kelvin-Helmhotz instabilities which arose from the relative motion between the ferrofluid and the air stream.

The criterion for instability in the magnetic Kelvin-Helmhotz problem when the ferrofluid film is under the action of a magnetic field is given by, [17]

$$(\bar{u} - u_\infty)^2 > \frac{\rho_f + \rho_a}{\rho_f\rho_a}\left[2\left[g_e(\rho_f - \rho_a)\sigma\right]^{\frac{1}{2}}\right] \tag{8}$$

where u_∞ is the air free stream velocity; ρ_f and ρ_a the density of the ferrofluid and the air, respectively; σ the surface tension; g_e is the effective normal acceleration resulting from all the volumetric forces acting on the fluid in that direction. Taking into account that $\rho_f \gg \rho_a$ and using Eq.(7), Eq.(8) can be rewritten as function of the interfacial velocity u_i as

$$\frac{u_i}{u_\infty} > \frac{3}{2}\left[1 + \frac{1}{u_\infty}\left[\frac{2\rho_f\sigma^{\frac{1}{2}}g_e^{\frac{1}{2}}}{\rho_a}\right]^{\frac{1}{2}}\right] \tag{9}$$

This effective gravity can be calculated as the superposition of gravity and the magnetic field applied normal

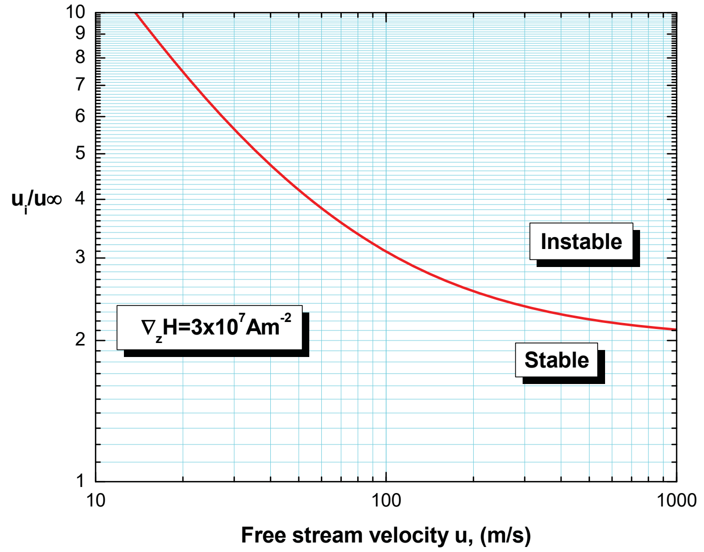

FIG. 3: Stability curve predicted by Eq.(12) as a function of the air free stream

to the surface. The volumetric magnetic force is given by [17]

$$f_m = \mu_o M \nabla_z H \tag{10}$$

where μ_o is the permeability of free space; M the magnetization of the ferrofluid, and $\nabla_z H$ is the gradient of the magnetic field normal to surface. Thus, the effective volumetric acceleration g_e may be defined as

$$g_e = g + \frac{\mu_o M \nabla_z H}{\rho_f} \tag{11}$$

where g is the earth gravity. Inserting Eq.(11) into Eq.(9) yields

$$\frac{u_i}{u_\infty} > \frac{3}{2}\left[1 + \frac{1}{u_\infty}\left[\frac{2\sigma^{\frac{1}{2}}(g\rho_f + \mu_o M \nabla_z H)^{\frac{1}{2}}}{\rho_a}\right]^{\frac{1}{2}}\right] \tag{12}$$

- **Discussion**

In order to obtain some idea o the shape of the curves predicted by Eq.(12), we assume some typical values of the parameters for a ferrofluid water based: $\sigma = 70\times10^{-3}$ N/m; $g = 9.8$ m/(s^2); $\rho_f = 1.2\times10^3$ kg/(m^3); $\rho_a = 1.0$ kg/(m^3); $M = 4.5\times10^5$ A/(m) which corresponds to a realizable magnetic field around 0.5 T obtained from a typical hand-held permanent magnet; $\mu_o = 4\pi\times10^{-7}$ H/(m). The resulting curve is shown in Fig. 3 considering practical achievable value for the magnetic gradient.

C. Experimental measurement

Because the purpose of the present work is a first assessment on the use of a ferrofluid moving thin film as active control flow strategy, and if it is allowable to assume that from an aerodynamic point of view the effect of the ferrofluid moving film can be regarded as similar than a moving wall, therefore, it is possible to use the available experimental data on the lift and attack angle enhancement resulting from moving walls with the same motion than the interface air-ferrofluid. If so, only will be necessary - as first estimate, to measure the interfacial velocity of the interface air-ferrofluid and from here extrapolate the result with that from a moving wall.

FIG. 4: Experimental setup

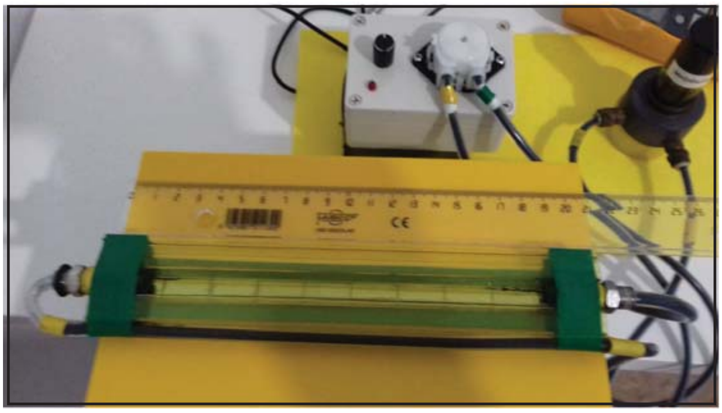

FIG. 5: Closeup of ferrofluid

With this goal, a set of experiments were performed in order to verify the interfacial velocity from the ferrofluid moving thin film.

Figs. 5 an 6 show the configuration for the series of experiments. A simple square polycarbonate cavity

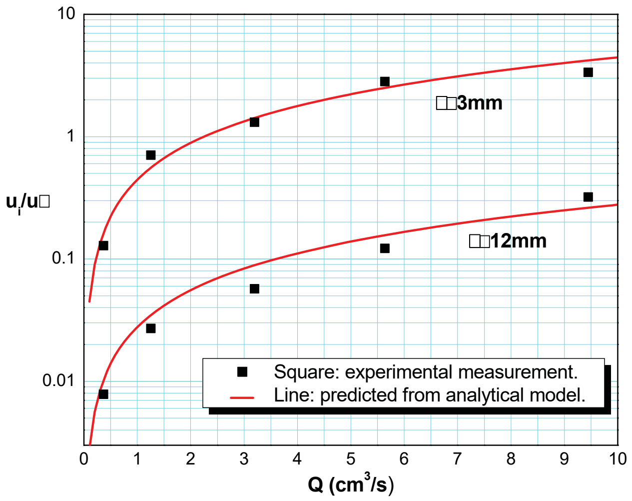

FIG. 6: $\frac{u_i}{u_\infty}$ as a function of the volumetric flow and for several thickness of the cavity and a free stream air velocity $u_\infty = 0.5$ m/s.

was used, i.e., $\delta = l$ with an open cavity 170-mm-long at the top filled with ferrofluid. A train of hand-held neodymium permanent magnets were attached at the bottom generating the normal magnetic field. A peristaltic pump with control on the number of revolution per minute was used to pump the ferrofluid through the cavity. Two cavities were employed keeping the same length but with widths $\delta = 3mm$ and $\delta = 12mm$. The ferrofluid was $Mn_{0.5}Zn0.5Fe_2O_4$ in water. The system was located in a wind tunnel where an air free stream was injected parallel to the cavity. Interfacial velocity u_i as function of several parameter (velocity of the air free stream, . The measurement of the air velocity was performed using a Fluke 922 airflow meter. The magnetic field from the array of magnets was 0.12 T at the wall and was measured with a FW BELL 5170 Gauss/Tesla meter.

III. RESULTS AND CONCLUSIONS

The resulting experimental curves are shown in Fig. 6 and Fig. 7. Fig. 6 shows the ratio $\frac{u_i}{u_\infty}$ as function of the volumetric flow (controlled by the number of revolution per minute of the peristaltic pump) and for the two cavities of 3mm and 12 mm with a stream velocity $u_\infty = 0.5$m/s. Fig. 7 shows the ratio $\frac{u_i}{u_\infty}$ as function of the free stream air.

Finally, from the experimental data reported on moving walls it is possible to asses the lift enhancement and delay of the detachment of the boundary layer (increase of the attack angle), this is because from a purely mechanical point of view, for very thin films, there are not differences if the motion of the interface is produced by a solid moving surface or from a fluid thin film. For illustration, Fig. 8 shows lift and attack angle enhancement for a NACA0015 which is derived from the experimental data on moving walls reported by [18]. The attractiveness of the proposed concept is easily to see by comparing the lift coefficient enhancement as function of $\frac{v_i}{u_o}$ from Fig. 10, and the allowable $\frac{u_i}{u_\infty}$ as function of the air stream velocity from the curve of ferrohydrodynamic stability, Fig. 3 Thus, as an example, an air stream velocity around 100 m/s, will allow for a thin film $\frac{u_i}{u_\infty}$ ratios around ≈ 3 m/s before Kelvin Helmholtz will detach the film. With these ratios, the lift coefficient enhancement could be around 1.8 which is figure of merit to be considered. Additional R&D is required in order to explore the possibilities in the use if ferrofluid thin films.

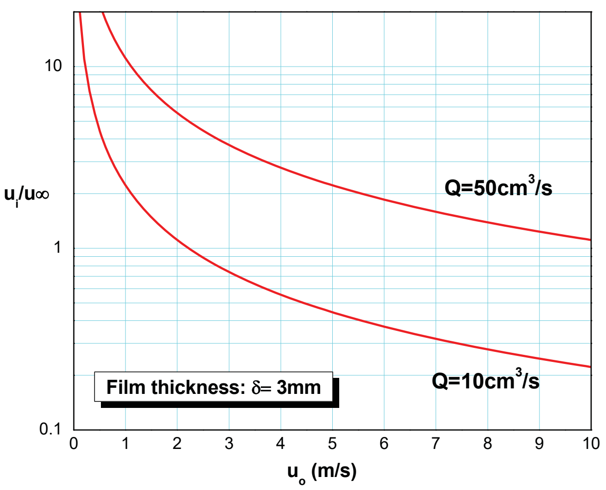

FIG. 7: $\frac{u_i}{u_\infty}$ as a function of the free stream air

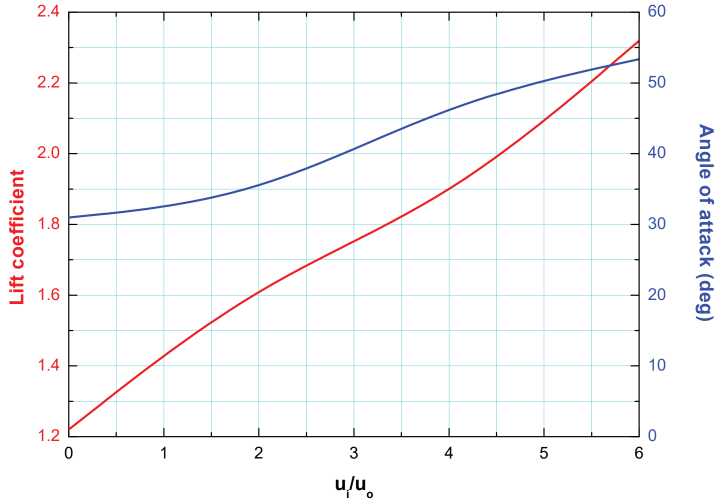

FIG. 8: Lift coefficient (left ordinate axis) Angle of Attack (right ordinate axis) as a function of $\frac{u_i}{u_\infty}$

- **Declaration of Interests**

The authors report no conflict of interest.

NOMENCLATURE

f_m = volumetric magnetic force
g = earth gravity
g_e = effective gravity
H = magnetic field
l = width of the ferrofluid film
M = magnetization
p = pressure
Q = volumetric flow
u = velocity of ferrofluid
$\bar{u}$ = average velocity of ferrofluid
u_∞ = stream air velocity
v = velocity of air
y = length co-ordinate
z = normal co-ordinate

Greek symbols

δ = thickness of the ferrofluid film
μ = dynamic viscosity
μ_o = permeability of free space
ρ = density
σ = surface tension

subscripts

a = air
f = ferrofluid
i = interface air-ferrofluid

ACKNOWLEDGEMENTS

This research was supported by the Spanish Ministry of Economy and Competitiveness under fellowship grant Ramon y Cajal: RYC-2013-13459.

[1] Qu X; Zhang Y; Lu X; Zhu J. 2020. Unsteady experimental and numerical investigation of aerodynamic performance in ultra-high-lift LPT Chinese Journal of Aeronautics. In press

[2] Qu X; Zhang Y; Lu X; Zhu J. 2019. Unsteady wakes-secondary flow interactions in a high-lift low-pressure turbine cascade Chinese Journal of Aeronautics. In press

[3] Tabatabaeian S; Mirzaei M; Sadighzadeh A; Damideh V; Shadaram A. 2012. Experimental Investigation of the Effects of Various Plasma Actuator Configurations on Lift and Drag Coefficients of a Circular Cylinder Including the Effects of Electrodes Chinese Journal of Aeronautics. Volume 25, Issue 3. Pages 311-324

[4] Wen Q; Guo A; Li H; Dong W. 2018. Nonlinear dynamics of a flapping rotary wing: Modeling and optimal wing kinematic analysis Chinese Journal of Aeronautics. Volume 31, Issue 5. Pages 1041-1052

[5] Abbas L.K; Qian C; Marzocca P; Zafer G; Mostafa A. 2008. Active Aerothermoelastic Control of Hypersonic Double-wedge Lifting Surface Chinese Journal of Aeronautics. Volume 21, Issue 1. Pages 8-18

[6] Zhou C; Zhang Y; Wu J. 2020. Effect of flexibility on unsteady aerodynamics forces of a purely plunging airfoil Chinese Journal of Aeronautics. Volume 33, Issue 1. Pages 88-101

[7] Szwaba R; Flaszynski P; Doerffer P. 2019. Streamwise vortex generation by the rod Chinese Journal of Aeronautics. Volume 32, Issue 8. Pages 1903-1911

[8] Han M; Li J; Niu Z; Liang H; Hua W. 2015. Aerodynamic performance enhancement of a flying wing using nanosecond pulsed DBD plasma actuator Chinese Journal of Aeronautics. Volume 28, Issue 2. Pages 377-384

[9] Lu Y; Wang C. 2015. Active control for performance enhancement of electrically controlled rotor Chinese Journal of Aeronautics. Volume 28, Issue 5. Pages 1494-1502

[10] Wu T; Song B; Song W; Yang W; Han Z. 2020. Aerodynamic performance enhancement for flapping airfoils by co-flow jet Chinese Journal of Aeronautics. In press

[11] Liu Z, Luo Z; Liu Q; Zhou Y. 2020. Modulation of driving signals in flow control over an airfoil with synthetic jet Chinese Journal of Aeronautics. In press

[12] Zhang X; Li H; Huang Y; Tang K; Wang W. 2019. Leading-edge flow separation control over an airfoil using a symmetrical dielectric barrier discharge plasma actuator. Chinese Journal of Aeronautics. 32, 5. p.p. 1190-1203

[13] Ma S; Chu W; Zhang H; Li X; Kuang H. 2019. A combined application of micro-vortex generator and boundary layer suction in a high-load compressor cascade. Chinese Journal of AeronauticsVolume 32, 5. p.p. 1171-1183

[14] Liu B; Liang H; Han Z; Li Y; Ding Z. 2020. Numerical research on airfoil transition delay by alternative current dielectric barrier discharge actuation. Chinese Journal of Aeronautics. . In press

[15] Ganesh N; Arunvinthan S; Pillai S.N. 2029. Effect of surface blowing on aerodynamic characteristics of tubercled straight wing Chinese Journal of AeronauticsVolume 32, Issue 5May 2019Pages 1111-1120

[16] Batchelor G.K 2000. An introduction to fluid dynamics. Cambridge university press, 2000. Cambridge University Press, 2000. 615 pages

[17] Rosenweig R.E. 1985. Ferrohydrodynamics. Dover publications, iInc, Mineola, New York.

[18] Boukenkoul M; Feng-Chen, Li; Wen-Li, Chen; Hong-Na, Zhang. 2017. Lift-generation and moving-wall flow control over a Low Aspect Ratio airfoil. Journal of Fluids Engineering. 140.